Can fusion, elastic and inelastic scattering of heavy ions be understood, without a simultaneous analysis of them?

To cite this article: R M Anjos *et al* 1997 *J. Phys. G: Nucl. Part. Phys.* **23** 1423

J. Phys. G: Nucl. Part. Phys. **23** (1997) 1423–1429. Printed in the UK PII: S0954-3899(97)85074-8

Can fusion, elastic and inelastic scattering of heavy ions be understood, without a simultaneous analysis of them?

R M Anjos†, C Muri, S B Moraes, R Cabezas‡, P R S Gomes, C Tenreiro§, R Liguori Neto‖, A M M Maciel and G M Santos

Instituto de Física, Universidade Federal Fluminense, Av. Litoranea s/n, Gragoatá, Niterói, RJ, 24210-340, Brazil

Received 13 June 1997

Abstract. We present examples of situations where the absence of a simultaneous analysis of the scattering and reaction mechanisms leads to an incomplete or even false understanding of these processes. The optical model analysis of the elastic scattering gives rise to different values of reaction cross sections, while the simple analysis of the fusion excitation functions may lead to ambiguous or wrong conclusions. Data for the $^{14}N+^{59}Co$ system obtained by our group is used in the analysis.

1. Introduction

The complexity of low-energy and short-distance colliding mechanisms, with strong coupling between them, leads to the need for a simultaneous description of the fusion, quasi-elastic reactions, elastic and inelastic scattering. The search for a unique nuclear potential that describes simultaneously different reaction mechanisms is, therefore, quite important for their understanding.

A suitable approach for the study of the fusion process is to consider the coupling of low-lying excited states of the colliding nuclei. The complexity of the full coupled-channel calculations has made widespread the use of approximations and simplified codes, such as the CCFUS [1], whilst for the study of the elastic scattering it is usual to use the optical model; these procedures lead to ambiguities. Another approach to the study of reaction and scattering processes is to replace the many channels theory by a one-dimensional barrier penetration model with an energy dependent optical potential [2].

In this paper we present new data for the elastic and inelastic scattering differential cross sections of the $^{14}N+^{59}Co$ system, at near barrier energies. The fusion excitation function for this system had been previously measured by our group [3]. Simultaneous fits of the three reactions were performed by coupled-channel calculations and energy dependent optical potentials. The analysis of the elastic scattering would be ambiguous without the strong constraint of the fusion cross section data. The conclusions from the previous analysis of the fusion excitation function by the simplified CCFUS code [3] were different from the

† Contact author: e-mail address: meigikos@if.uff.br
‡ Fellow of the Centro Latino Americano de Física-CLAF.
§ Permanent address: Facultad de Ciencias, Universidad de Chile, Santiago 1, Chile.
‖ Permanent address: Instituto de Física, Universidade de São Paulo, São Paulo, Brazil.

0954-3899/97/101423+07$19.50

ones obtained by the ECIS [4] and FRESCO [5] codes, when the potentials are deduced from elastic and inelastic data.

We also show original fusion cross section data for the ^{9}Be+^{64}Zn system, leading to the same compound nucleus as the ^{14}N+^{59}Co. The aim is to investigate the influence of the break-up of the ^{9}Be on the fusion process. The study is not yet conclusive, due to the lack of elastic scattering data for this system.

The experiments were performed at the 8UD Pelletron accelerator of the University of São Paulo. The fusion cross sections were measured by the gamma-ray spectroscopy method [3]. The elastic and inelastic scattering angular distributions were measured with the use of an array of eight silicon surface barrier detectors [6]. The experimental set-up and details will not be presented in this paper.

2. Optical model analysis

The optical model, with a Wood–Saxon potential, was used in a first approach for the analysis of the elastic scattering data. All the calculations were performed by using the code ECIS. When one makes the search of the optimum sets of optical model parameters (OMP) by fitting just the elastic angular distributions, many families of OMP are obtained. Examples of the ambiguities are shown in table 1. Sets of OMP with similar χ^2, leading to different reaction cross section values, fit the elastic angular distributions equally well. The fits of any of these sets are represented by the full lines of figure 1.

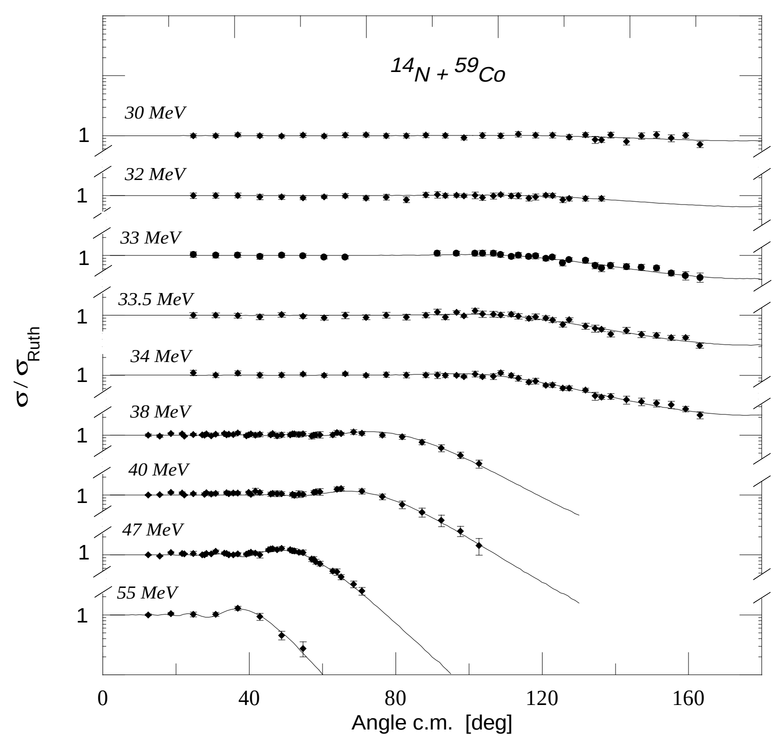

Figure 1. Elastic scattering angular distributions for the ^{14}N + ^{59}Co reactions. The lines show the best fits from the optical model and coupled-channel calculations.

Table 1. Examples of optical potential parameters that fit the elastic scattering angular distributions, shown in figure 1, leading to different reaction cross sections.

E_{Lab} (MeV)		V (MeV)	W (MeV)	$R_v = R_w$ (fm)	$a_v = a_w$ (fm)	χ^2/N	σ_{reaction} (mb)
	set 1	51.15	5.45	1.25	0.60	0.50	15.06
30.0	set 2	123.8	1.19	1.25	0.50	0.46	8.77
	set 3	161.1	7.07	1.15	0.60	0.50	11.50
	set 1	46.22	13.65	1.15	0.65	0.55	45.04
32.0	set 2	25.64	3.0	1.25	0.65	0.58	37.6
	set 3	110.6	28.7	1.25	0.55	0.55	43.73
	set 1	61.99	3.59	1.25	0.50	0.66	71.36
33.0	set 2	39.81	4.12	1.20	0.65	0.68	69.94
	set 3	16.80	1.24	1.30	0.65	0.64	61.23
	set 1	89.02	2.04	1.15	0.60	0.83	75.7
33.5	set 2	14.6	1.95	1.30	0.65	0.86	88.6
	set 3	57.86	3.59	1.25	0.50	0.85	91.99
	set 1	5.06	2.24	1.45	0.50	0.76	150.2
34.0	set 2	127.3	12.0	1.15	0.55	0.79	126.7
	set 3	40.61	3.59	1.25	0.55	0.81	123.4
	set 1	61.06	8.85	1.25	0.50	0.40	424.1
38.0	set 2	58.90	3.59	1.25	0.50	0.45	404.6
	set 3	21.53	6.59	1.25	0.65	0.41	430.7
	set 1	55.20	8.05	1.25	0.50	0.73	531.6
40.0	set 2	16.71	9.51	1.25	0.65	0.76	563.3
	set 3	10.53	5.71	1.30	0.65	0.75	551.0
	set 1	32.39	10.59	1.25	0.55	0.91	875.8
47.0	set 2	47.50	9.59	1.25	0.50	0.88	860.9
	set 3	23.60	9.21	1.25	0.60	0.96	882.5
	set 1	51.40	10.2	1.25	0.50	0.31	1156
55.0	set 2	35.68	11.0	1.25	0.65	0.28	1172
	set 3	12.74	6.76	1.30	0.65	0.28	1222

However, when the experimental fusion cross sections were used as a strong constraint, most of the ambiguities could be removed. The fusion cross sections were calculated by the code FRESCO, using different sets of parameters obtained by the fit to the elastic scattering data. Simultaneous fits of the elastic angular distributions and the fusion cross sections were obtained. Some ambiguities, however, were still present, since for each of the four diffuseness values, from 0.50 fm to 0.65 fm, one real and one imaginary strength were derived for each energy. These four families of OMP fit equally well the elastic scattering angular distribution and the fusion cross section with a $\chi^2/N_{\text{points}} < 1$. For all of them, the values of real potential depth reached a maximum at the lowest energies, where one expects to find the threshold anomaly.

3. Inelastic scattering analysis: coupled-channel calculations

The inclusion of the inelastic scattering in the analysis was made by a coupled-channel treatment, using the ECIS code. The ^{59}Co(^{14}N,^{14}N)^{59}Co($3/2^-$; 1.098 MeV) data were measured in the energy range 30 MeV $\leqslant E_{\text{Lab}} \leqslant$ 34 MeV. The ^{14}N was considered as spherical. For the description of the ^{59}Co, we have considered it to be a ‘single-hole’ nucleus, in which the unpaired particle is a proton in the 1f$_{7/2}$ sub-shell, bound to a deformed, axially symmetric core. A description based on the rotational model was employed. The initial coupling scheme considered only one excited state of the target. When the second excited state was also considered, no significant influence on the elastic and the inelastic angular distributions was observed. Furthermore, the influence of the reorientation terms was shown to be negligible.

Optical potentials determined by fitting elastic scattering distributions and fusion excitation functions were used to generate the coupling potentials. Reasonable fits were obtained for the values of the quadrupole deformation parameters $\beta_{2V} = \beta_{2W} = 0.0718$ and $\beta_{2C} = 0.0724$. During the χ^2 search, the real and the imaginary strength V_0 and W_0 were varied, keeping fixed the geometry obtained in the optical model fitting ($R_{0V} = R_{0W} = 1.25$ fm and $a_V = a_W = 0.60$ fm). An energy independent potential with $V_0 = 28.8$ MeV and $W_0 = 3.59$ MeV was derived. The results of the fits of the inelastic scattering are shown in figure 2. The fits for the elastic scattering and fusion are superposed with those shown in figures 1 and 3, respectively.

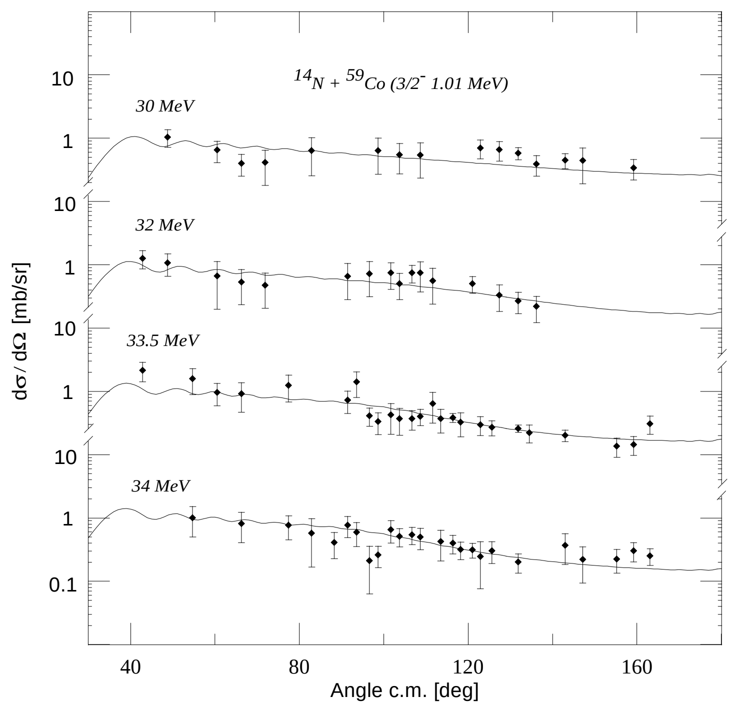

Figure 2. Inelastic scattering angular distributions for the first excited state in ^{59}Co, at 1.098 MeV. Full curves represent the best fits obtained from the coupled-channel analysis of the data.

Therefore, the inclusion of the coupling of the first excited state of the ^{59}Co inelastic channel leads to the complete loss of the anomalous energy dependence of the potential at low energies. This result is clear evidence that both the threshold anomaly and the coupling of inelastic channels have the same effect on the fusion and elastic scattering processes. The first excited state of the target, for this system, is the only channel that plays an important role in the coupling scheme. If the contributions of other channels were relevant, the energy dependence of the potential would still remain.

4. Fusion excitation function analysis

Our group had previously measured [3] the fusion excitation function for the $^{14}N + ^{59}Co$ system, at bombarding energies from 32–56 MeV. The analysis was performed by simplified coupled-channel calculations, using the CCFUS code. The results indicated that the effect of the coupling of inelastic channels was not enough to explain the fusion cross section enhancement at low energies. This could be obtained only if transfer channels were also included in the calculations. Scattering data were not available at that time.

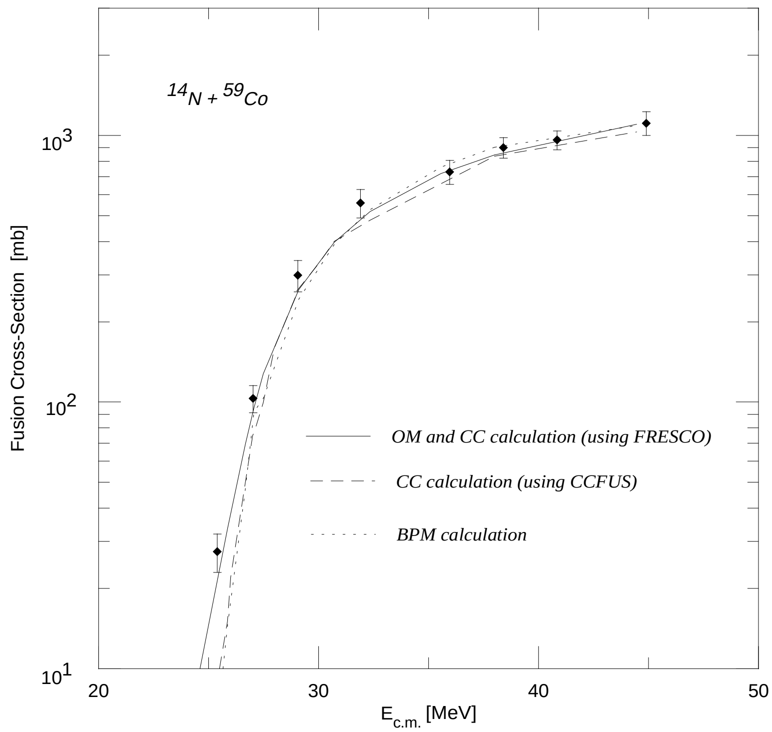

Figure 3. Fusion cross sections for the $^{14}N+^{59}Co$ system. The points represent the experimental data. The full curve represents the predictions using the potentials deduced from the optical model and coupled-channel calculations analysis. The broken curve is the result obtained with the CCFUS code. The dotted curve corresponds to the predictions of the one-dimensional barrier penetration model either by CCFUS code or by the FRESCO code.

Figure 3 shows the fusion excitation function for this system, for the present and previous analyses. The dotted curve is the prediction of the one-dimensional barrier penetration model calculated by the code FRESCO. The full curve shows the fusion cross sections predicted by the optical model and by the coupled-channel method. All the fusion cross section calculations were performed by the code FRESCO. As the experimental fusion cross sections were also used in the derivation of the potentials based on the fits of the elastic and inelastic angular distributions, a simultaneous fit of the three processes was obtained. The near barrier fusion behaviour for this system is, therefore, explained either by the coupling of inelastic channels or by the presence of the threshold anomaly. The results from the previous analysis are shown by the broken line of figure 3. The predictions of the

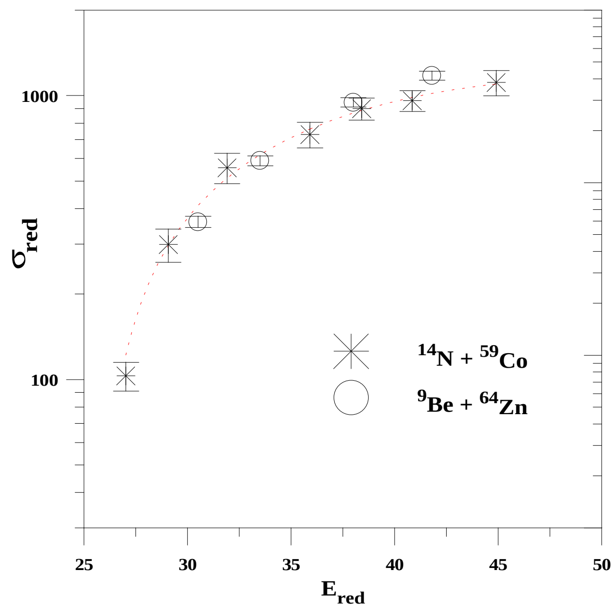

Figure 4. Reduced fusion excitation function for the $^{14}N + ^{59}Co$ and $^{9}Be + ^{64}Zn$ systems.

uncoupled barrier penetration model from these calculations are similar to the ones obtained by the code FRESCO.

5. The influence of the break-up process on the fusion

We are investigating the influence of the break-up on the fusion process, at near barrier energies, for reactions induced by ^{9}Be on medium heavy targets, like ^{64}Zn. The compound nucleus formed, ^{73}Se, is the same as for the $^{14}N + ^{59}Co$ system. The excitation energies and angular momenta are within the same range for both systems. The small separation energies for the ^{9}Be ($S_n = 1.67$ MeV) favours the break-up process. A recent paper [7] suggests that the fusion of light systems is inhibited by the break-up process on weakly bound nuclei. For the two systems that we studied, however, a plot of their reduced fusion excitation functions, as shown in figure 4, indicates that the break-up of the ^{9}Be does not inhibit the fusion cross section. It is possible that the break-up process is an extra channel that enhances the reaction cross section. This hypothesis could be tested only if there were elastic scattering data available for that system.

6. Summary and conclusions

Our message is that one cannot understand a single reaction mechanism, at near barrier energies, without a simultaneous analysis of all the important processes that are coupled with it. Separate analyses have been widely performed so far. We have shown examples of uncertainties on the reaction cross sections, coming from the analysis of the scattering data, which are removed with the simultaneous analysis of the fusion data. Also, the analysis of the fusion excitation function is not enough to understand unambiguously its behaviour and the influence of other reaction mechanisms on it.

It is specially important to remark that the use of simplified coupled-channel calculations based on codes such as CCFUS may lead to qualitative conclusions different from those obtained from full coupled-channel calculations. The code CCFUS has advantages such as its simplicity and the possibility of performing coupled-channel calculations without any other experimental information apart from the fusion data. A clear comparison between the predictions of the ECIS/FRESCO and CCFUS codes should be done only if they use the same kind of potentials.

Acknowledgment

The authors would like to thank the Conselho Nacional de Desenvolvimento Científico e Tecnlógico-CNPq, for their financial support.

References

[1] Dasso C H, Landowne S and Winther A 1983 *Nucl. Phys.* A **405** 381
Dasso C H and Landowne S 1987 *Phys. Lett.* **183B** 141
[2] Nagarajan M A, Mahaux C and Satchler G R 1985 *Phys. Rev. Lett.* **54** 1136
Nagarajan M A and Satchler G R 1986 *Phys. Lett.* **173B** 29
Satchler G R 1991 *Phys. Rep.* **199** 147
[3] Gomes P R S *et al* 1991 *Nucl. Phys.* A **534** 429
Gomes P R S, Penna T J P, Liguori Neto R, Acquadro J C, Tenreiro C, Freitas P A B, Crema E, Carlin Filho N and Coimbra M M 1989 *Nucl. Instr. Meth. Phys. Res.* **280** 395
[4] Raynal J 1989 ECIS 88 Code *Proc. Workshop on Applied Nucl. Theory and Nucl. Model Calculations for Nucl. Technology Applications (Trieste)* (Singapore: World Scientific) p 506
[5] Thompson I J, Comp. 1988 *Phys. Rep.* **7** 167
[6] Tenreiro C, Acquadro J C, Freitas P A B, Liguori Neto R, Ramirez G, Cuevas N, Gomes P R S, Anjos R M and Copnell J 1996 *Phys. Rev.* C **53** 2870
[7] Takahashi J, Munhoz M J, Szanto E M, Carlin N, Added N, Suaide A A P, Moura M M, Liguori Neto R and Szanto de Toledo A 1997 *Phys. Rev. Lett.* **78** 30